Analytical treatment of constraints in fragmentation

A. J. Cole
Laboratoire de Physique Subatomique et Cosmologie, Université Joseph Fourier CNRS-IN2P3, 53 Avenue des Martyrs, 38026 Grenoble, Cedex, France
(Received 29 July 2003; published 28 May 2004)

In fragmentation of a finite object such as an atomic nucleus or a percolation lattice, the multidimensional probability distribution of the numbers of fragments of each mass (charge, size) may be approximated as a product of Poisson distributions. In this work we present an analytical treatment of the influence of constraints (multiplicity, mass, etc.) that may be imposed on the basic product distribution.

DOI: 10.1103/PhysRevC.69.054613 PACS number(s): 25.70.Pq, 25.70.Mn, 24.60.Ky

I. INTRODUCTION

When a finite nucleus breaks into fragments the simplest observation consists in measuring the average numbers of fragments of mass (m) or charge (z). In this work, we refer to these quantities as $\langle n_m \rangle$. It should, however, be understood that, despite the systematic use of the word "mass" the analysis presented herein also applies to fragment charges and to other manifestations of fragmentation such as the sets of fragments produced in bond percolation simulations. For a discussion of nuclear fragmentation we refer the reader to the recent review by Richert and Wagner [1] and to references therein. A detailed discussion of statistical models for fragmentation can be found in Refs. [2–4].

An experiment carried out with a sophisticated multidetector is capable of measuring the set of fragment masses (more usually charges) event by event. Each event is then represented by a vector $\mathbf{n} \equiv \{n_1, n_2, \ldots, n_m, \ldots\}$ $(n_m \geqslant 0)$. The multiplicity is defined as $\Sigma_m n_m$ and the experiment provides an estimate of the partition probabilities. If the total mass of the fragmenting object is known (M) then $\mathbf{n}$ represents a partition of the integer M and the sum rule $\Sigma_{m=1}^{M} m n_m = M$ applies. We shall write sums and products over m, respectively, as Σ_m and Π_m.

A model for partition weights (or probabilities) $W(\mathbf{n})$ [or $P(\mathbf{n})$] may be readily constructed using only the average values $\langle n_m \rangle$. The interest is twofold. First, to the extent that the model provides a "reasonable" description of the available data, it provides estimations of other interesting observables. Second, it serves as a basis for the development of more sophisticated model structures which may be necessary to explain nontrivial correlations in the production of fragments.

The basic model considered herein results from the assumption of absence of correlations, i.e.,

$$W(\mathbf{n}) = \prod_m w_m(n_m). \tag{1.1}$$

The model is developed by the specification of the individual distributions $w_m(n_m)$ as correctly normalized Poisson factors

$$p_m(n_m) = \frac{[X_m]^{n_m} e^{-X_m}}{n_m!}, \tag{1.2}$$

in which each of the parameters X_m (collectively referred to as $\mathbf{X}$ or the set $\{X_m\}$) is equal (by definition) to the corresponding mean value $\langle n_m \rangle$. We note that models of this "generic" type have met with considerable success in reproducing results of multifragmentation experiments [5–8]. The specific problem of correlations in small systems was discussed by Cole and Désesquelles [9].

The specification made in Eq. (1.2) obviously implies that the sum of partition probabilities $\Sigma_{\mathbf{n}} P(\mathbf{n};\mathbf{X}) = 1$. However, if the multiplicity and total mass can be considered as constraints (N, M) this is no longer the case. We write the formal expression

$$\sum_{\mathbf{n}} P(\mathbf{n};\mathbf{X},N,M) \equiv \sum_{\mathbf{n}} \prod_m \frac{[X_m]^{n_m} e^{-X_m}}{n_m!} \delta\left(\sum_m n_m - N\right) \times \delta\left(\sum_m m n_m - M\right) < 1. \tag{1.3}$$

The constraints themelves introduce correlations. Thus, in the presence of constraints, $\langle n_m \rangle$ is no longer equal to X_m and quantities such as $\langle n_i n_j \rangle - \langle n_i \rangle \langle n_j \rangle$ are usually nonzero for all pairs of indices (i, j).

This work concerns the analytical treatment of a particular set of constraints which may be imposed on the basic distribution of probabilities $P(\mathbf{n};\mathbf{X})$. The constraints considered are multiplicity, total mass, and higher order moments of the same form. Thus an arbitrary choice of moments $\Sigma_{m=1}^{M} m^k n_m$ can be constrained to the values κ_k (with this notation $N = \kappa_0$ and $M = \kappa_1$). The primary goal will be to provide a version of Eq. (1.3) in which the delta functions no longer appear. The essential formalism will be developed in the following section. In Sec. III, the analytical result is validated by a comparison of predictions for mass distributions (for a few multiplicities) with results of Monte Carlo calculations. In this section we also compare the prediction of the partition probability density, as a function of κ_2, for fixed values of N and M, with the simulation result.

In Sec. IV, we begin by an extension of the formalism which is used to demonstrate that, in the case of multiplicity and mass constraints, the probability distribution $p(n_m)$ for the number of fragments of mass m is correctly reproduced. This leads naturally to a study of the inverse problem, i.e., obtaining the set $\{X_m\}$ from the set of mean values $\langle n_m \rangle$.

In Sec. V, we examine the joint probability distribution $p(n_i, n_j)$ corresponding to multiplicity and mass constrained

partitions with n_i fragments of mass i and n_j fragments of mass j, and in Sec. VI we derive and test identities which associate mean values and higher moments of the constrained fragment number distribution (quantities such as $\langle n_i \rangle$ and $\langle n_i n_j \rangle$) with specific members of the probability distribution itself. These identities are exact characteristics of the multinomial distribution. Remarks and conclusions are presented in Sec. VII.

II. THE CONSTRAINED PROBABILITY

It is, in principle, possible to (numerically) generate all partitions corresponding to the product Poisson distribution selecting those that satisfy a given set of constraints. The difficulty of this enterprise can be appreciated by making a rough evaluation. Let us suppose the values of the parameters X_m are such that the probabilities for any n_m to be greater than or equal to 10 can be discarded. Under these circumstances, denoting the highest value of m for which $X_m > 0$ as M_T, the number of partitions to be examined is of the order of 10^{M_T}. Of course, one can use Monte Carlo techniques to provide an estimation of probabilities, but for small probabilities such calculations become extremely time consuming and eventually impossible. We are therefore justified in seeking an alternative strategy.

The following derivation is based on a technique used to obtain level densities in atomic nuclei [10]. We first make the Laplace transform of the sum of constrained probabilities and then make the inverse transform using an approximation to the exact integrand. The $(K+1)$-dimensional Laplace transform of the sum of constrained probabilities is

$$\begin{aligned} Z(\boldsymbol{\alpha}) &= \sum_{\mathbf{n}} \int_0^\infty \int_0^\infty \cdots \int_0^\infty P(\mathbf{n};\mathbf{X}) \left\{ \prod_k \delta\left(\sum_m m^k n_m - \kappa_k \right) \right\} \\ &\quad \times e^{-\alpha_0 \kappa_0} e^{-\alpha_1 \kappa_1} \cdots e^{-\alpha_K \kappa_K} d\kappa_0 d\kappa_1 \cdots d\kappa_K \\ &= \sum_n P(\mathbf{n};\mathbf{X}) e^{-\Sigma_k \alpha_k \Sigma_m m^k n_m}, \end{aligned} \tag{2.1}$$

in which the symbol Σ_k designates the sum $\Sigma_{k=0}^K$. We now note that

$$e^{-\Sigma_k \alpha_k \Sigma_m m^k n_m} = e^{-\Sigma_m n_m \Sigma_k \alpha_k m^k} = \prod_m [e^{-\Sigma_k \alpha_k m^k}]^{n_m}. \tag{2.2}$$

Then, recalling the normalized form for the partition probability [Eqs. (1.1) and (1.2)] and writing the configuration sum as $\Sigma_{\mathbf{n}} \equiv \Sigma_{n_1} \Sigma_{n_2} \cdots \Sigma_{n_m} \cdots$, we obtain

$$\begin{aligned} Z(\boldsymbol{\alpha}) &= e^{-\Sigma_m X_m} \sum_{n_1} \frac{[X_1 e^{-\Sigma_k \alpha_k 1^k}]^{n_1}}{n_1!} \times \sum_{n_2} \frac{[X_2 e^{-\Sigma_k \alpha_k 2^k}]^{n_2}}{n_2!} \\ &\quad \times \cdots \times \sum_{n_m} \frac{[X_m e^{-\Sigma_k \alpha_k m^k}]^{n_m}}{n_m!} \times \cdots. \end{aligned} \tag{2.3}$$

We recognize that the second and subsequent factors on the right hand side of Eq. (2.3) are simple expansions of exponentials so that, finally,

$$Z(\boldsymbol{\alpha}) = \prod_m e^{X_m [e^{-\Sigma_k \alpha_k m^k} - 1]} \tag{2.4}$$

and (explicitly exhibiting the limit M_T)

$$\ln[Z(\boldsymbol{\alpha})] = \sum_{m=1}^{M_T} X_m [e^{-\Sigma_k \alpha_k m^k} - 1]. \tag{2.5}$$

The inverse Laplace transform will now be evaluated approximately, thus providing an approximation to $\Sigma_{\mathbf{n}} P(\mathbf{n};\mathbf{X},\boldsymbol{\kappa})$ which we will refer to as $Q(\mathbf{X},\boldsymbol{\kappa})$. The exact transform is, of course,

$$\begin{aligned} \sum_{\mathbf{n}} P(\mathbf{n};\mathbf{X},\boldsymbol{\kappa}) &= \left[\frac{1}{2\pi i} \right]^{K+1} \int_{c_0 - i\infty}^{c_0 + i\infty} \int_{c_1 - i\infty}^{c_1 + i\infty} \cdots \int_{c_K - 1\infty}^{c_K + i\infty} Z(\boldsymbol{\alpha}) \\ &\quad \times e^{\Sigma_k \alpha_k \kappa_k} d\alpha_0 d\alpha_1 \cdots d\alpha_K. \end{aligned} \tag{2.6}$$

We now define $f(\boldsymbol{\alpha}) = \ln[Z(\boldsymbol{\alpha})] + \Sigma_k \alpha_k \kappa_k$ and replace the integrand in Eq. (2.6) by the exponential of the second order Taylor expansion of $f(\boldsymbol{\alpha})$ about the point $\boldsymbol{\alpha} = \mathbf{a}$ defined by the set of equations $df/d\alpha_k = 0$ $(k = 0, K)$. Making the change of variables $\alpha_k = c_k + i\upsilon_k$ (when $\boldsymbol{\alpha} = \mathbf{a}$, let $\boldsymbol{\upsilon} = \mathbf{u}$) we approximate the inverse Laplace transform as

$$Q(\mathbf{X},\boldsymbol{\kappa}) = \frac{e^{f(\mathbf{a})}}{(2\pi)^{K+1}} \int_{-\infty}^{+\infty} \int_{-\infty}^{+\infty} \cdots \int_{-\infty}^{+\infty} e^{g(\boldsymbol{\upsilon})} d\upsilon_0 d\upsilon_1 \cdots d\upsilon_K \tag{2.7}$$

in which $g(\boldsymbol{\upsilon})$ is defined by the expansion

$$\begin{aligned} f(\boldsymbol{\alpha}) - f(\mathbf{a}) &\approx \sum_{i=0}^K \sum_{j=0}^K \frac{(\alpha_i - a_i)(\alpha_j - a_j)}{2!} \left. \frac{d^2 f}{d\alpha_i d\alpha_j} \right|_{\boldsymbol{\alpha} = \mathbf{a}} \\ &= \sum_{i=0}^K \sum_{j=0}^K \frac{(\upsilon_i - u_i)(\upsilon_j - u_j)}{2!} \left. \frac{d^2 f}{d\upsilon_i d\upsilon_j} \right|_{\boldsymbol{\upsilon} = \mathbf{u}}. \end{aligned} \tag{2.8}$$

The integral in Eq. (2.7) is well known [2,11] and yields

$$Q(\mathbf{X},\boldsymbol{\kappa}) = \frac{e^{f(\mathbf{a})}}{(2\pi)^{(K+1)/2}} \times \frac{1}{\sqrt{\det(f'')}}, \tag{2.9}$$

where the symmetric square matrix f'' has elements

$$f''_{i,j} = \left. \frac{d^2 \ln[Z(\boldsymbol{\alpha})]}{d\alpha_i d\alpha_j} \right|_{\boldsymbol{\alpha} = \mathbf{a}}. \tag{2.10}$$

To complete the derivation we need only write down the first and second derivatives of $f(\boldsymbol{\alpha})$. The minimum satisfies

$$\left. \frac{df}{d\alpha_i} \right|_{\boldsymbol{\alpha} = \mathbf{a}} = -\sum_{m=1}^{M_T} X_m m^i e^{-\Sigma_k a_k m^k} + \kappa_i = 0 \tag{2.11}$$

and, at the minimum,

$$\left. \frac{d^2 \ln[Z(\boldsymbol{\alpha})]}{d\alpha_i d\alpha_j} \right|_{\boldsymbol{\alpha} = \mathbf{a}} = \sum_{m=1}^{M_T} X_m m^{i+j} e^{-\Sigma_k a_k m^k}. \tag{2.12}$$

An example of the application of these equations will be given in the next section, in which we begin by obtaining an expression for Q under constraints of mass and multiplicity.

III. CASE STUDY: MULTIPLICITY, MASS, AND κ_2 CONSTRAINTS

Referring back to Eq. (1.3), let us select the part of the probability for which the total multiplicity $\kappa_0=N$ and the total mass $\kappa_1=M$. No other constraints apply. In this case we can divide the two equations [(2.11), with $i=0,1$] to obtain

$$\frac{M}{N}=\frac{\sum_m X_m m e^{-a_1 m}}{\sum_m X_m e^{-a_1 m}}. \tag{3.1}$$

The (numerical) solution of this equation for a_1 can then be used to obtain a_0. Thus, using the multiplicity equation [(2.11) with $i=0$] we obtain

$$a_0=\ln\left[\frac{\sum_m X_m e^{-a_1 m}}{N}\right]. \tag{3.2}$$

The determinant in Eq. (2.9) can be calculated straightforwardly using Eq. (2.12). We define

$$S_i \equiv \sum_m X_m m^i e^{-\Sigma_k a_k m^k} \tag{3.3}$$

and further write

$$\sigma=\left[\frac{S_2}{N}-\frac{M^2}{N^2}\right]^{1/2}. \tag{3.4}$$

The result is simply

$$\det[f'']=N^2\sigma^2. \tag{3.5}$$

Then, recalling the expression for Q [Eq. (2.9)] (where no confusion can arise we will supress the argument $\mathbf{X}$) we obtain

$$\ln[Q(N,M)]=N-\sum_m X_m+a_0N+a_1M-\ln[2\pi N\sigma]. \tag{3.6}$$

In order to test Eq. (3.6) we consider a specific case in which X_m is defined as a sum of exponentials, i.e., $X_m=A_1e^{-\gamma_1 m}+A_2e^{-\gamma_2 m}$ for $m=1,\ M_T$. The parameters ($A_1=1.0,\ \gamma_1=0.1,\ A_2=35,\ \gamma_2=1.0,\ M_T=80$) were chosen to provide mean values $\langle n_m\rangle$ which are not unlike results of percolation simulations and multifragmentation experiments in the vicinity of the phase transition [12]. An unconstrained Monte Carlo generation of partititions using this distribution yields a mean multiplicity of 30 and a mean mass of 131. We constrained the multiplicity to take on a few values around this mean and compared distributions of Q, for an appropriate range of masses, with Monte Carlo estimates obtained by generating partitions using the unconstrained Poisson product probability distribution and recording the fraction of partitions with the specified values of N and M. The results are shown in Fig. 1. The agreement is most gratifying and perhaps even a little surprising. Eventually, of course, statistical precision becomes a limitation in the Monte Carlo simulations. However, within the range of statistical errors, the results do not reveal any significant discrepancy. As a further test we have calculated the constrained partition probability density as a function of κ_2 for fixed values $N=30$ and $M=130$. The straightforward generalization of Eq. (3.6) leads, in this case to the expression

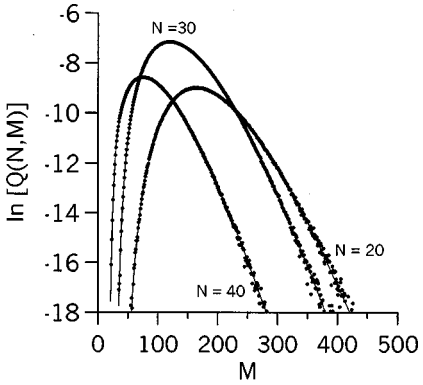

FIG. 1. Constrained probabilities $Q(N,M)$ [Eq. (3.6)] compared with results of Monte Carlo simulations (filled circles) with $X_m=e^{-0.1m}+35e^{-m}$ for $1\leqslant m\leqslant 80$ ($X_m=0, m>80$). The predictions are represented as continuous lines.

$$\ln[Q(N,M,\kappa_2)]=N-\sum_m X_m+a_0N+a_1M+a_2\kappa_2 - 0.5\ln[8\pi^3\Delta], \tag{3.7}$$

where the determinant Δ is given as

$$\Delta=N\kappa_2S_4-NS_3^2+2M\kappa_2S_3-M^2S_4-\kappa_2^3. \tag{3.8}$$

The comparison with the Monte Carlo simulation, shown in Fig. 2, is generally satisfactory but reveals a discrepancy for high values of κ_2 (albeit for probabilities of the order of 10^{-7}). A detailed investigation reveals that this discrepancy is simply due to the limitation of the quadratic approximation [Eq. (2.8)] with respect to the variable α_2 (the difficulty does not occur for smaller values of κ_2). For estimation of low order moments of the distribution of κ_2 the difficulty can be

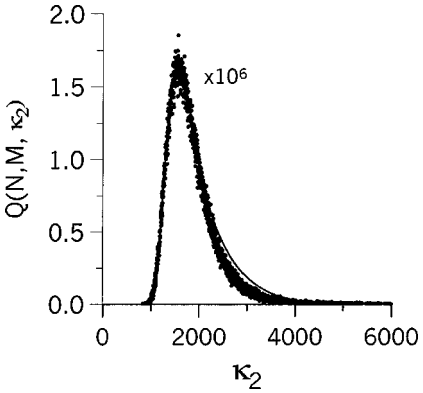

FIG. 2. Probability distributions [Eq. (3.7)] of the second moment κ_2 for fixed values of the multiplicity N (30) and total mass M (130). Other specifications as in Fig. 1. Note that if N is even (odd) κ_2 is even (odd) so that the (continuous) approximation must be multiplied by a factor of 2 before comparing with data.

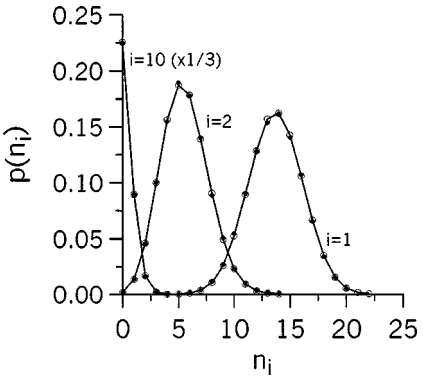

FIG. 3. Probability distributions corresponding to the numbers of fragments of mass i ($i=1$, 2, and 10). In each case the quantity displayed is $p(n_i)=W(n_i)/Q(N,M)$ with $W(n_i)$ given by Eq. (4.1). The Monte Carlo calculations are represented as filled circles and the predictions by open circles joined by straight lines (set $\{X_m\}$ as in Fig. 1, $N=30$, $M=130$).

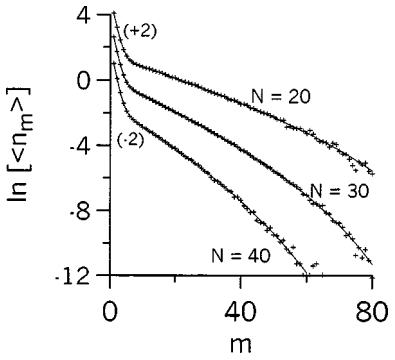

FIG. 4. Predicted mean values $\langle n_m\rangle$ [Eq. (4.2)] compared with Monte Carlo simulation results ($M=130$, $N=20,30,40$). The Monte Carlo "data" are represented by crosses and the predictions by straight lines (set $\{X_m\}$ as in Fig. 1). Values for $N=20$ and $N=40$ have been displaced by +2 and −2, respectively.

circumvented by direct use of the moments $\langle n_i\rangle$ and $\langle n_i\cdot n_j\rangle$ (calculated using only multiplicity and mass constraints), which, as shown in the following sections, can be estimated accurately.

IV. CONSTRAINED FRAGMENT SIZE DISTRIBUTIONS

We will be concerned, in this section, with partitions constrained by multiplicity and total mass. The generalization to include constraints of higher order is straightforward. With multiplicity and mass constraints the statistical weight associated with partitions for which the number of fragments of mass i is equal to n_i, when expressed using the Laplace transform approximation, can be written

$$W(n_i)=\frac{[X_i]^{n_i}e^{-X_i}}{n_i!}\sum_{\mathbf{n}}\prod_m\frac{[X_m^{(i)}]^{n_m}e^{-X_m^{(i)}}}{n_m!}\delta\Big(\sum_m n_m-(N-n_i)\Big)\times\delta\Big(\sum_m mn_m-(M-in_i)\Big)\approx\frac{[X_i]^{n_i}e^{-X_i}}{n_i!}Q(\mathbf{X}^{(i)},(N-n_i),(M-in_i)),\tag{4.1}$$

where the set of parameters $\mathbf{X}^{(i)}\equiv\{X_m^{(i)}\}$ is identical with the set $\{X_m\}$ with the exception of the parameter X_i, which is removed. Using the set $\{X_m\}$ defined in the previous section, with $N=30$ and $M=130$, we show in Fig. 3 the prediction provided for the distribution of the numbers of fragments of mass 1, 2, and 10. As can be seen there is no observable discrepancy with the simulation results.

The mean value $\langle n_m\rangle$ *within* the subset constrained by mass and multiplicity is

$$\langle n_m\rangle=\frac{\sum_{n_m}n_mW(n_m)}{\sum_{n_m}W(n_m)}.\tag{4.2}$$

Using Eq. (4.1), the sum in the denominator of Eq. (4.2) is simply $\Sigma_{n_m}W(n_m)=Q(N,M)$.

We show in Fig. 4, for three multiplicities, the predicted $\langle n_m\rangle$ distributions compared with the Monte Carlo calculations. This figure demonstrates (at least in the case considered) that, provided the set $\{X_m\}$ is given, the theory accurately predicts the resulting set of values of $\langle n_m\rangle$.

In practice, of course, one is faced with the inverse problem. The experiment measures a set of average partial multiplicities $\langle n_m\rangle$, and the first step for application of the multinomial theory is to obtain the set $\{X_m\}$. In the presence of constraints this involves a multidimensional nonlinear search procedure. An alternative procedure, which has been used in this work, is based on the fact that a change in the parameter X_m mainly influences the corresponding $\langle n_m\rangle$ value. Using Eq. (4.1) and noting that $Q(\mathbf{X}^{(m)},(N-n_m),(M-mn_m))$ does not depend on X_m, we easily obtain

$$\frac{dW(n_m)}{dX_m}=W(n_m)\left(\frac{n_m}{X_m}-1\right).\tag{4.3}$$

Now, from Eq. (4.2)

$$\frac{d\langle n_m\rangle}{dX_m}=\frac{\sum_{n_m}n_m\left[\frac{dW(n_m)}{dX_m}\sum_{n_m}W(n_m)-W(n_m)\sum_{n_m}\frac{dW(n_m)}{dX_m}\right]}{\left[\sum_{n_m}W(n_m)\right]^2},\tag{4.4}$$

and on inserting Eq. (4.3) we find the exact relation

$$\frac{d\langle n_m\rangle}{dX_m}=\frac{\langle n_m^2\rangle-\langle n_m\rangle^2}{X_m},\tag{4.5}$$

so that

$$\frac{d\ln[\langle n_m\rangle]}{d\ln[X_m]}=\frac{\langle n_m^2\rangle-\langle n_m\rangle^2}{\langle n_m\rangle}\equiv\frac{\sigma^2(n_m)}{\langle n_m\rangle}.\tag{4.6}$$

Consider first the case for $m>M/2$, for which n_m can take on only the values 0, 1, so that only the weights $W(0)$ and $W(1)$ are nonzero. Equation (4.6) then reduces to

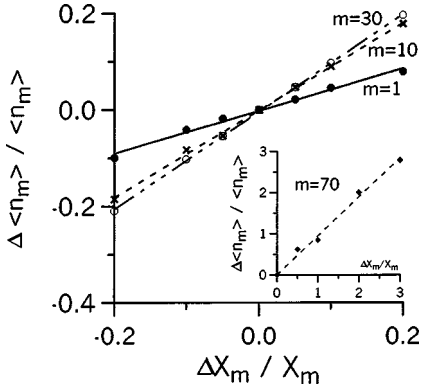

FIG. 5. Monte Carlo simulation results obtained by variation of X_m parameters. For each value of m the variation was made starting with the set **X** specified in the caption to Fig. 1 [see Eq. (4.8) and preceding text]. The straight lines represent linear least squares fits to the Monte Carlo "data."

$$\frac{d\ln[\langle n_m\rangle]}{d\ln[X_m]} = 1 - \langle n_m\rangle. \tag{4.7}$$

More generally, one observes that the variance $\sigma^2(n_m)$ increases *almost* linearly with the mean value $\langle n_m\rangle$ (these quantities are identical for the Poisson distribution). Thus, as shown in Fig. 5, the relation

$$\Delta\ln[n_m] = C(m)\times\Delta\ln[X_m] \tag{4.8}$$

holds approximately for all m with $C(m)\leqslant 1$. Equation (4.8) provides a basis for a search routine which, in a given cycle, successively modifies each value of Xm and generally converges after a few such cycles.

We show in Fig. 6 the result of the search procedure applied to the $\langle n_m\rangle$ distribution obtained from the Monte Carlo simulation using the double exponential distribution specified just after Eq. (3.6). We mention in passing that, as remarked by Désesquelles [13], the set $\{X_m\}$ obtained for fixed N and M may be transformed, using arbitrary constants y and

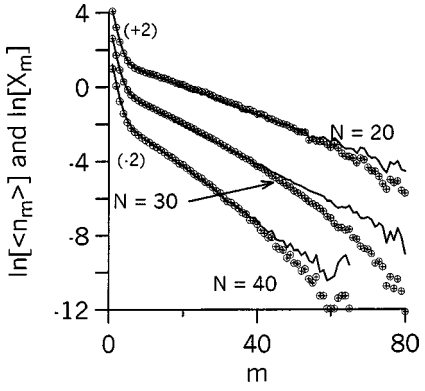

FIG. 6. Results of search procedure: $\langle n_m\rangle$ values ($M=130$, $N=20,30,40$) obtained from the Monte Carlo simulations are represented by crosses and predictions (the final values obtained from the search routine) as open circles. The X_m values obtained from the search routine are represented as continuous lines. Values for $N=20$ and $N=40$ have been displaced by +2 and −2, respectively.

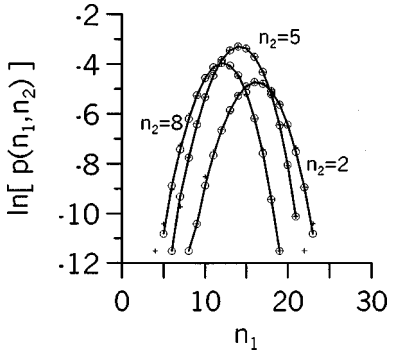

FIG. 7. Probability [defined within the subset with $N=30$ and $M=130$, Eq. (5.1)] to simultaneously observe n_i fragments of mass i and n_j fragments of mass j with $i=1$ and $j=2$. The Monte Carlo results are represented by crosses and the predictions, by open circles joined by straight lines (set $\{X_m\}$ as in Fig. 1).

z, to the set $\{X_m yz^m\}$ with no effect on observables. In the present context the only consequence is that two values selected from the set $\{X_m\}$ can be fixed *a priori* in the search procedure. Figure 6 demonstrates that the search procedure is successful insofar as the Monte Carlo $\langle n_m\rangle$ distributions are nicely reproduced.

V. TWO FRAGMENT CORRELATIONS

In this section we briefly discuss two fragment correlations within the subset of partitions constrained by multiplicity and mass. The probability of observing events within this subset with n_i fragments of mass i and n_j fragments of mass j is obtained as an obvious extension of Eq. (4.1), i.e.,

$$p(n_i,n_j) = \frac{W(n_i,n_j)}{\sum_{n_i,n_j} W(n_i,n_j)} = \frac{W(n_i,n_j)}{Q(N,M)}, \tag{5.1}$$

where

$$\begin{aligned} W(n_i,n_j) = {} & \frac{[X_i]^{n_i}e^{-X_i}}{n_i!}\times\frac{[X_j]^{n_j}e^{-X_j}}{n_j!}\sum_{\mathbf{n}}\prod_m \frac{[X_m^{(i,j)}]^{n_m}e^{-X_m^{(i,j)}}}{n_m!} \\ & \times\delta\Big(\sum_m n_m - (N-n_i-n_j)\Big) \\ & \times\delta\Big(\sum_m m n_m - (M-in_i-jn_j)\Big) \\ \approx {} & \frac{[X_i]^{n_i}e^{-X_i}}{n_i!}\times\frac{[X_j]^{n_j}e^{-X_j}}{n_j!} \\ & \times Q(\mathbf{X}^{(i,j)},(N-n_i-n_j),(M-in_i-jn_j)). \end{aligned} \tag{5.2}$$

The results of calculations using this formula are compared with Monte Carlo simulations in Figs. 7 and 8. The Monte Carlo results (obtained from simulations with 10^9 events) are limited by statistics. However, within these limitations the predictions appear to be rather accurate.

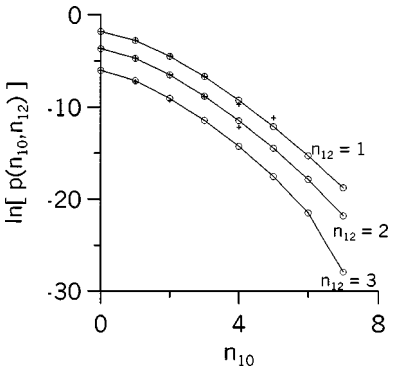

FIG. 8. As Fig. 7 but for $i=10$ and $j=12$.

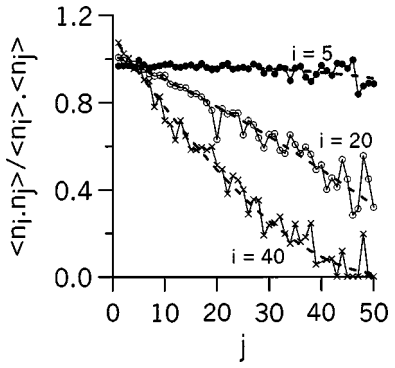

FIG. 9. Correlation ratios. The results of the Monte Carlo simulations (10^8 events, set $\{X_m\}$ as in Fig. 1, $N=30$, $M=130$) are represented as filled circles, open circles, and crosses linked by thin straight lines. The predictions [Eq. (6.5)] are represented as thick dashed lines. Diagonal elements (which would be off scale in this figure) have been suppressed.

VI. CHARACTERISTIC IDENTITIES

There are several ways to obtain the identities to be presented in this section. The present derivation makes use of equations presented previously. We can begin with the mean value $\langle n_i\rangle$ which, by deriving Eq. (1.3) with respect to X_i, can be written

$$\frac{\langle n_i\rangle}{X_i}=1+\frac{1}{P(\mathbf{X},N,M)}\frac{dP(\mathbf{X},N,M)}{dX_i}. \tag{6.1}$$

The derivative can be obtained from Eq. (2.6). We first note that $d\ln[Z(\boldsymbol{\alpha})]/dX_i=e^{-\alpha_0-\alpha_1 i}-1$. Then, differentiating the integrand, we obtain

$$\begin{aligned}\frac{dP(\mathbf{X},N,M)}{dX_i}&=\left[\frac{1}{2\pi i}\right]^2\int_{c_0-i\infty}^{c_0+i\infty}\int_{c_1-i\infty}^{c_1+i\infty}Z(\boldsymbol{\alpha})\\&\quad\times e^{\alpha_0 N+\alpha_1 M}(e^{-\alpha_0-\alpha_1 i}-1)d\alpha_0 d\alpha_1\\&\equiv P(\mathbf{X},N-1,M-i)-P(\mathbf{X},N,M).\end{aligned} \tag{6.2}$$

The identity

$$\frac{\langle n_i\rangle}{X_i}=\frac{P(\mathbf{X},N-1,M-i)}{P(\mathbf{X},N,M)} \tag{6.3}$$

follows immediately. Similarly, we may readily obtain

$$\frac{\langle n_i n_j\rangle}{X_i X_j}=\frac{P(\mathbf{X},N-2,M-i-j)}{P(\mathbf{X},N,M)} \tag{6.4}$$

and thereby the correlation ratio

$$\frac{\langle n_i n_j\rangle}{\langle n_i\rangle\langle n_j\rangle}\approx\frac{Q(\mathbf{X},N-2,M-i-j)Q(\mathbf{X},N,M)}{Q(\mathbf{X},N-1,M-i)Q(\mathbf{X},N-1,M-j)}, \tag{6.5}$$

which for independent emission would be identically equal to unity for all off-diagonal elements. Monte Carlo calculations of this ratio together with predictions provided by Eq. (6.5) are shown in Fig. 9. Once again the calculations successfully reproduce the Monte Carlo data. The departure from unity observed in the figure is mainly due to constraint of the total mass. Relations such as Eq. (6.5) should be of considerable value in exploring the pertinence of the constrained multinomial approximation.

VII. CONCLUDING REMARKS

In this work we developed a simple technique for evaluating probabilities associated with the constrained multinomial model. We have shown, in a case study designed to produce observables similar to those observed in nuclear multifragmentation, that the technique produces predictions which generally provide an excellent description of results obtained from Monte Carlo simulations. The technique is expected to be especially useful for estimation of small probabilities or, more importantly, of ratios of small probabilities which cannot be easily estimated by simulation.

It is useful to note that the basic model structure considered herein is reproduced in at least one of the currently successful statistical models for nuclear multifragmentation [3] (see also [8,13]). On the other hand, in many physical situations one may expect departures from predictions of the multinomial model due to the dynamical processes involved in multifragmentation [14]. In this case, the Laplace transform method can be used as a basis (a sort of null hypothesis) that should facilitate detection and characterization of such processes.

[1] J. Richert and P. Wagner, Phys. Rep. **350**, 1 (2001).
[2] A. J. Cole, *Statistical Models for Nuclear Decay* (IOP, Bristol, 2000).
[3] J. P. Bondorf, A. S. Botvina, A. S. Iljinov, I. N. Mishustin, and K. Sneppen, Phys. Rep. **257**, 133 (1995).
[4] D. H. E. Gross, *Microcanonical Thermodynamics*, World Scientific Lecture Notes in Physics Vol. 66 (World Scientific, Singapore, 2001).
[5] A. J. Cole, P. J. Lindstrom, H. J. Crawford, and B. G. Harvey, Phys. Rev. C **39**, 891 (1989).
[6] P. Désesquelles, A. J. Cole, A. Giorni, D. Heuer, A. Lleres, J. B. Viano, B. Chambon, B. Cheynis, D. Drain, and C. Pastor, Phys. Rev. C **48**, 1828 (1993).
[7] P. Kreutz *et al.*, Nucl. Phys. **A556**, 672 (1993).
[8] A. J. Cole *et al.*, Z. Phys. A **356**, 171 (1996).
[9] A. J. Cole and P. Désesquelles, Z. Phys. A **337**, 71 (1990).
[10] T. Ericson, Adv. Phys. **9**, 425 (1960).
[11] Y. Suzuki and K. Varga, *Stochastic Variational Approach to Quantum Mechanical Few-Body Problems* (Springer, Heidelberg, 1998).
[12] M. D'Agostino *et al.*, Phys. Lett. B **371**, 175 (1996); Nucl. Phys. **A650**, 329 (1999).
[13] P. Désesquelles, Phys. Rev. C **65**, 034604 (2002).
[14] A. Guarnera, M. Colonna, and P. Chomaz, Phys. Lett. B **373**, 267 (1996); P. Chomaz, M. Colonna, A. Guarnera, and B. Jaquet, Nucl. Phys. **A583**, 305c (1995).